Scalar relaxation of NMR transitions at ultralow magnetic field

Michael C. D. Tayler[a,*], Lynn F. Gladden[a]

[a]*Department of Chemical Engineering and Biotechnology, University of Cambridge, Philippa Fawcett Drive, Cambridge, CB3 0AS, UK.*

Abstract

Nuclear magnetic resonance signals for ^{1}H in simple chlorinated, brominated and deuterated liquids were detected at field strengths between 1 nT and a few μT to investigate the influence of scalar relaxation of the second kind (SR2K). SR2K describes the acceleration in magnetization decay rate for a spin-1/2 nucleus that is scalar coupled to a fast-relaxing quadrupolar nucleus. In agreement with simple theoretical models, the experimental data show that couplings to nuclei with small, nonzero quadrupole moments (^{2}H) give rise to higher transverse relaxation rates at ultralow field than rapidly relaxing quadrupolar nuclei (Cl and Br). This behavior is opposite to the case normally encountered in high-field NMR, and demonstrates that certain nuclei in the spin system may be "weakly coupled" or even decoupled when the applied magnetic field is zero. The results show that the capability for precision determination of NMR frequencies and molecular structural information depends strongly on the composition and topology of the nuclear spin system.

Keywords: Ultralow-field NMR, Relaxation, Quadrupolar nuclei, Spin-spin coupling

1. Introduction

Ultralow magnetic field – where the magnitude of nuclear Larmor frequencies are comparable to those of inter-nuclear couplings – harbors a distinct regime of spin dynamics that underpins many valuable techniques in solution-state nuclear magnetic resonance (NMR) spectroscopy: (i) precision measurements of spin couplings down to an uncertainty of millihertz, due to a reduced inhomogeneous broadening proportional to field strength, and long natural coherence times[1, 2]; (ii) a high sensitivity to binding events and adsorption at surfaces, since nuclear spin relaxation times may depend strongly on intermolecular dynamics[3]; (iii) transfer of spin polarization from one nucleus to another via level anticrossings. Currently there is a strong research interest in these areas following the popularization of sensitive magnetometers as NMR detectors[4, 5, 6, 7] and the tremendous potential of spin hyperpolarization to enhance NMR sensitivity[8, 9, 10, 11].

A great concern in these areas is the influence of quadrupolar nuclei, where the spin quantum number is > 1/2 (e.g. [2]H, ^{14}N, [17]O [35/37]Cl, [79/81]Br). In the liquid state, scalar relaxation of the second kind (SR2K)[12] becomes a mechanism to accelerate the decay of spin polarization and coherences. SR2K involves the coherent flow of polarization from spin-1/2 nuclei into multi-spin-order terms between spin-1/2 and quadrupolar nuclei, via the scalar coupling interaction. These coherences may be quenched rapidly if the quadrupole interaction is large and/or the nucleus has a large spin quantum number, for the coherences are not spontaneously returned into populations of the spin-1/2 nuclei. SR2K can be highly detrimental to the amplitude and line width of NMR signals [13, 14]. On the other hand, SR2K is known to yield information about scalar couplings to the quadrupolar nuclei and the magnitude of quadrupole coupling constants[15, 16, 17, 18], providing insights into molecular electronic structure that cannot be probed directly.

Theoretical models are widely used in attempts to understand the behavior of SR2K[12, 19]. Consider the longitudinal ($1/T_1$) and transverse ($1/T_2$) rate contributions for a spin system comprising two nuclei "I" and "S" with respective total angular momentum quantum numbers $I = 1/2$, $S > 1/2$. Redfield theory assumptions are used to obtain the expressions

$$\frac{1}{T_1^{(I)}} = \frac{8\pi^2 J_{IS}^2}{3} \frac{S(S+1)T_2^{(S)}}{1+(\gamma_I - \gamma_S)^2 B_z^2 (T_2^{(S)})^2}, \quad (1)$$

*Corresponding author
    Email address:* `mcdt2@cam.ac.uk` (Michael C. D. Tayler)

$$\frac{1}{T_2^{(\text{I})}} = \frac{4\pi^2 J_{IS}^2 S(S+1)}{3}T_1^{(\text{S})} + \frac{1}{2T_1^{(\text{I})}}. \tag{2}$$

Here J_{IS} is the spin-spin scalar coupling between the nuclei (in Hz), $\gamma_{I/S}$ are the nuclear gyromagnetic ratios and B_z is the strength of the external magnetic field. A derivation is provided in Appendix A. These equations assume the extreme narrowing limit and that the S spin relaxes much faster than the I spin.

The purpose of this paper is to discuss SR2K at low magnetic fields where $|\gamma_I - \gamma_S|B_z T_2^{(\text{S})} \ll 1$. In this limit, Equations 1 and 2 simplify to

$$\frac{1}{T_1^{(\text{I})}} = \frac{1}{T_2^{(\text{I})}} = \frac{8\pi^2 J_{IS}^2 S(S+1)}{3}T_2^{(\text{S})}, \tag{3}$$

hence, an inverse dependence between the I and S relaxation rates is expected. Scalar relaxation at low field is expected to be least efficient when $T_2^{(\text{S})}$ is short. This contrasts with SR2K in high magnetic fields where $1/T_1^{(\text{I})} \propto 1/T_2^{(\text{S})}$. Despite the apparent opposite dependence on $T_2^{(\text{S})}$, however, both limits describe relaxation in a "weak coupling" regime where – for a given molecule at any instant in time – differences between spin state energies greatly exceed the magnitude of the scalar coupling constant. It is noted that inverse relationships between the relaxation rates of two spin species (e.g. Equation 3) do exist in certain cases of magnetic resonance in high field. One case is SR2K involving ^{13}C and ^{79}Br[17], where the nuclear gyromagnetic ratios differ by less than 0.4% and the difference in Larmor frequencies is small compared to $1/T_2^{(\text{S})}$ even at fields $B \sim 1$ T. Another case is nuclear relaxation due to hyperfine couplings with strongly paramagnetic lanthanide-III shift reagents[21], where a short electron $T_2^{(\text{S})}$ allows high spectral resolution to be maintained in the NMR spectra.

Zero-field NMR signals are acquired at magnetic fields where oscillations in the sample magnetization occur at J coupling frequencies. Observable signals only arise if there are at least two distinct nuclear spin species that are coupled together, where the coupling constant is faster than the relaxation rate of both nuclei. In a three-spin-species system IXS that has respective spin quantum numbers $I = X = 1/2$, $S > 1$ and relaxation rates $T_1^{(\text{S})} \ll T_1^{(\text{I})}$ and $T_1^{(\text{X})}$ the zero-field NMR spectrum is expected to contain a single resonance at the coupling frequency J_{IX}. The relaxation rate of the signal coherence is predicted to be

$$\frac{1}{T^{(\text{IX})}} = 2\pi^2(J_{IS}^2 + J_{XS}^2)S(S+1)T_2^{(\text{S})}, \tag{4}$$

which is also derived in Appendix A. This expression is very similar to Equation 3, differing only in the numerical factor as a result of the number of spins giving rise to the coherence.

In the following, simple experiments assess the impact of SR2K on NMR spectral line widths at ultralow field in chlorinated, brominated and deuterated organic compounds. The data qualitatively agree with the above theoretical predictions and prior work that has focused on magnetic resonance relaxation measurements of SR2K at much higher fields. In the light of these results, the validity of Equations 3 / 4 and the underlying theory is discussed.

2. Experimental methods

Upper bounds for SR2K rate contributions were estimated from ^{1}H magnetic resonance line widths of the following liquids at ultralow magnetic field: [1,2]-dichloroethane ($C_2H_4Cl_2$), [1,2]-dibromoethane ($C_2H_4Br_2$), [1,1,2,2]-tetrabromoethane ($C_2H_2Br_4$), [$^{13}C_1$]-bromoacetic acid ($^{13}CH_2BrCOOH$), ethanol-D (CD_3CH_2OD), [1,1]-deuterioethanol (CH_3CD_2OH) and [2,2,2]-trideuterioethanol (CD_3CH_2OH). Control measurements were made for similar compounds without quadrupolar nuclei: n-heptane (C_7H_{16}), [$^{13}C_1$]-acetic acid ($^{13}CH_3COOH$) and ethanol (CH_3CH_2OH).

Sample preparation: Compounds were sourced from a chemicals supplier (deuterated ethanols from CDN Isotopes, all others from Sigma Aldrich). Chemical purities of the liquid samples were checked to be $> 98\%$ via ^{1}H, ^{2}H or ^{13}C NMR at 1.4 T (60 MHz ^{1}H frequency). For each sample a 0.2 mL volume of liquid was transferred into a 5 mm outer diameter, 5 cm long NMR tube. The sample tubes were then degassed (freeze-pump-thaw), purged with carbon dioxide and flame sealed.

Ultralow-field NMR spectroscopy: NMR spectra were acquired inside a Mu-metal magnetic shield (Twinleaf LLC, model MS-1F) using a rubidium magnetometer (spin exchange relaxation-free ^{87}Rb vapor, 150 °C, measurement bandwidth 100 Hz). As the instrument has been described in other work[7], only a brief description is given here. Before each measurement the sample is held in the field of a 1.95 T NdFeB magnet, which is located outside the shield, for prepolarization. The sample tube is then quickly (<300 ms) brought into position next to the magnetometer. During this time a 1.0 mT magnetic field is applied to adiabatically orient the sample magnetization parallel to the sensitive axis of the magnetometer. The field is then rapidly switched off (<1 ms) and a transverse field (of magnitude B_x) applied

for precession, resulting in a time-dependent magnetometer signal proportional to $\cos(\gamma_I B_x t) \exp(-t/T_2^{*(H)})$. This signal is digitally sampled in the time domain (4000 Hz sampling rate, 16-bit resolution), zero filled, Fourier transformed and phase corrected to give the NMR spectrum. The critically important spin-exchange relaxation-free (SERF [20]) regime of magnetometer sets an upper limit for B_x and determines the temperature of the Rb vapor. In its current configuration, the magnetometer can measure NMR signals in bias fields up to $B_x \approx 2.4\,\mu$T ([1]H Larmor frequency of ~100 Hz) at 150 °C. The temperature of the sample throughout the measurement is approximately 40 °C. A factor in choosing the liquid samples is a boiling point of at least 40 °C above the measurement temperature, to avoid pressure buildup inside the sealed tubes.

3. Results

3.1. ^{1}H NMR of chlorinated and brominated ethanes

Free-precession ^{1}H NMR signals were recorded at bias magnetic fields of ~23.5 nT (1.0 Hz [1]H Larmor frequency) to ~2.35 μT (99 Hz [1]H Larmor frequency). Absorptive Lorentzian curves were fit to the phased spectral peaks to obtain the width at half height $= 1/\pi T_2^*$.

NMR spectra for $C_2H_4Cl_2$, $C_2H_4Br_2$ and $C_2H_2Br_4$ are shown in Figure 1. The data show increasing NMR peak widths between 20 Hz and 99 Hz ^{1}H precession frequencies due to instrument-specific gradients in the bias field ($\delta B_x/B_x \approx 2000$ ppm across the diameter of the sample). At precession frequencies 20 Hz or less the gradient-induced broadening appears negligible. Field shimming along the x, y and z axes of the magnetometer does not reduce the line width, thus in this limit $T_2^* \equiv T_2$.

The spectra for the n-heptane sample are considered a control, as the molecules do not contain quadrupolar nuclei. The peak width of 0.17 Hz ($1/T_2^* = 0.054$ s^{-1}) is the largest of all the molecules studied. Narrower natural line widths are observed for the halogenated ethanes. In the case of $C_2H_4Br_2$ and $C_2H_4Cl_2$ the spectral peak is exceptionally narrow with less than 0.07 Hz width at half height ($1/T_2^{*(I)} < 0.022$ s^{-1}). The reduction in peak width is consistent with a lower [1]H-^{1}H dipole-dipole contribution to the relaxation rate and a shorter correlation time for molecular tumbling resulting from the highly prolate moment of inertia tensor of the molecules. Furthermore, the contribution from the SR2K mechanism due to the presence of Cl or Br spin species appears completely negligible. This agrees with Equation 3 given typical literature values

[15] of $T_2^{(Cl)} < 10\,\mu$s, $^2J_{HCl} < 7$ Hz and $T_2^{(Br)} \ll 1\,\mu$s, $^2J_{HBr} < 15$ Hz that predicts line width contributions in the sub 10 mHz range.

3.2. ^{1}H NMR of partially deuterated ethanols

Deuterium, on the other hand, may impart a strong SR2K contribution to ^{1}H relaxation rates at ultralow field despite relatively weak coupling constants J_{HD} on the order of 1 or 2 Hz[22]. In general the H-D coupling is lower than the value of the corresponding H-H coupling by a factor of ~6.5, which is the ratio γ_D/γ_H. Figure 2 shows ^{1}H NMR spectra for isotopologs CH_3CH_2OH, CH_3CH_2OD, CD_3CH_2OH and CH_3CD_2OH. Respective peak widths at 10 Hz Larmor frequency are fit to (0.16 ± 0.01) Hz, (0.17 ± 0.01) Hz, (2.0 ± 0.1) Hz and (2.4 ± 0.1) Hz. The ^{1}H peak broadens significantly upon deuteration of the alkyl chain; the broadest peak for CH_3CD_2OH is more than one order of magnitude larger than for the non-deuterated sample.

The ^{2}H NMR spectra of the CD_3CH_2OH and CH_3CD_2OH samples at 1.4 T (9.15 MHz, 37 °C) each displays a resolved multiplet pattern (1:2:1 triplet and 1:3:3:1 quartet, respectively) at the C-D chemical shift. These splittings give a value for the H-D scalar coupling constant $^3J_{HD} = (1.03 \pm 0.01)$ Hz. Inversion-recovery relaxation measurements for CD_3CH_2OH at 1.4 T also yield $T_1^{(D)} = 1.2 \pm 0.1$ s and $T_1^{(H)} = 3.8 \pm 0.1$ s. If it is true that the relaxation rates do not vary with field, these data show $|1/T_2^{(D)} - 1/T_2^{(H)}| \ll 2\pi J_{HD}$ and that the main assumption leading to Equation 3 may be violated, namely that the two isotopic species are not weakly coupled. Simple perturbation theory may therefore not accurately predict the transverse relaxation rate. For instance, if the experimental values of J and $T_2^{(D)}$ are used in Equation 3, the CD_3CH_2OH sample ought to yield $1/T_2^{*(H)} = 16\pi^2 J_{HD}^2 T_2^{(D)} \approx 160$ s^{-1}, which is over one order of magnitude larger than the observed relaxation rate. To be consistent with the perturbation model the $T_2^{(D)}$ at ultralow field must be on the order of 30-40 ms. Either this is caused by other sources of relaxation (e.g. dipole-dipole couplings) that are not accounted for in the model, or another explanation must be found. A plausible reason for the broad line width is rapid relaxation of the coherences via multi-spin-order (described by, e.g. $S_{\pm}S_z$ spin operators), which can be populated as the result of strong coupling between the two spin species.

3.3. Zero-field NMR of [2-^{13}C]-bromoacetic acid

NMR in zero field, where the magnetic background is highly uniform and the detected signals are long-lived zero-quantum coherences[24], provides a route
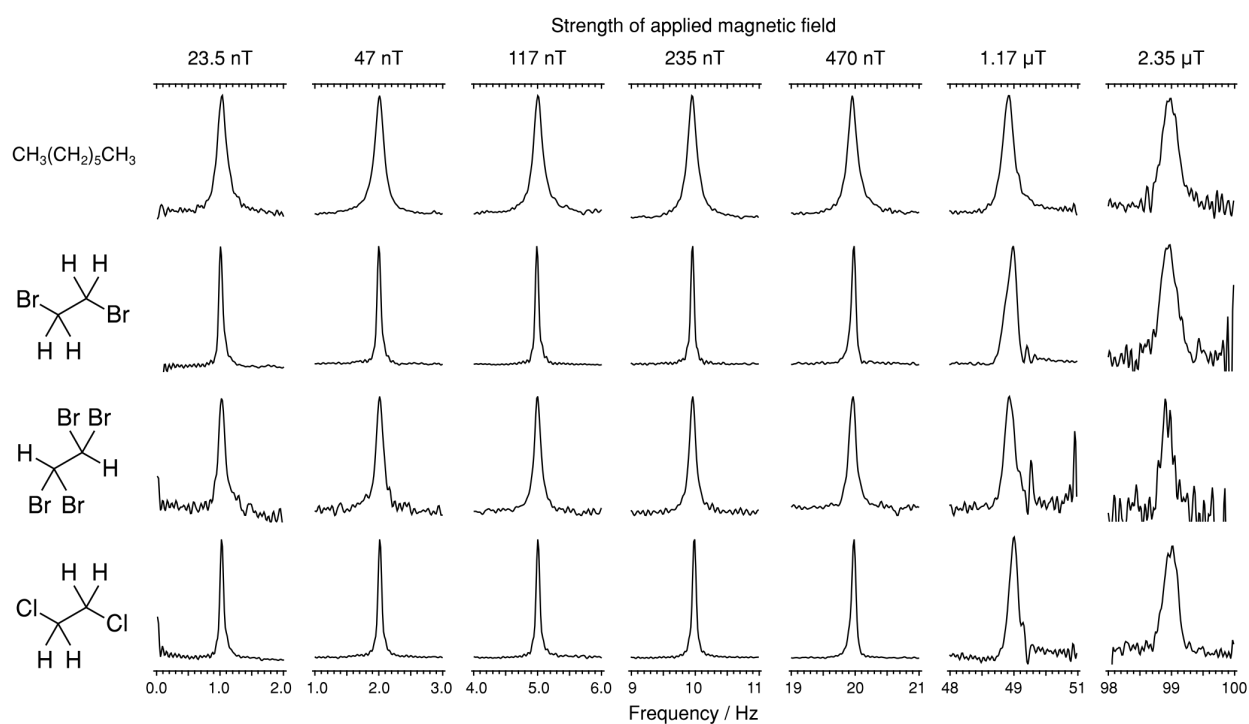
3

Figure 1: In-phase ultralow-field ^{1}H NMR spectra of n-heptane and halogenated ethanes in neat liquid form. The horizontal axis gives the absolute signal frequency and the width of each displayed region is 2.0 Hz. The expected ^{1}H Larmor frequency at the quoted value of magnetic field B_x is given by $\gamma_H B_x$ where $\gamma_H \approx 42.5775$ Hz/μT is the ^{1}H gyromagnetic ratio. Below 470 nT, field-gradient-induced broadening of the NMR signals appears negligible. At 1.0 Hz ^{1}H Larmor frequency the full peak widths at half maximum are fit to: 0.17 Hz (C_7H_{16}); 0.070 Hz ($C_2H_2Br_4$); 0.12 Hz ($C_2H_4Br_2$); 0.067 Hz ($C_2H_4Cl_2$).
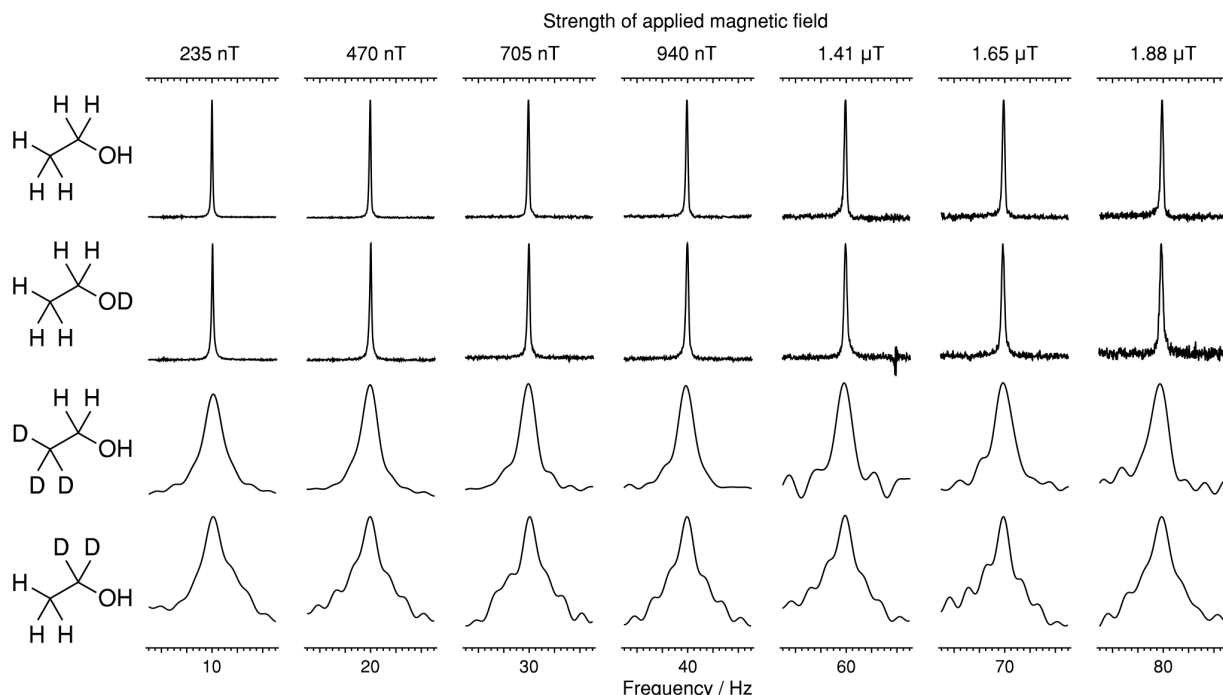
Figure 2: In-phase ultralow-field ^{1}H NMR spectra of neat ethanol, ethanol-d, [2,2,2]-trideuterioethanol and [1,1]-deuterioethanol (top to bottom). The horizontal axis gives the absolute signal frequency and the width of each displayed region is 10.0 Hz. At 10.0 Hz ^{1}H Larmor frequency the peak widths at half maximum are fit to 0.16 Hz (CH$_3$CH$_2$OH) 0.17 Hz (CH$_3$CH$_2$OD); 2.0 Hz (CD$_3$CH$_2$OH) and 2.4 Hz (CH$_3$CD$_2$OH).

to obtain precise measurements of spin-spin scalar couplings[25, 26, 27]. The question arises: "is high resolution obtained when molecules contain rapidly relaxing quadrupolar nuclei?"

To examine the effect of SR2K on zero-field NMR peak widths the compound [2-^{13}C]-bromoacetic acid (^{13}CH$_2$BrCOOH) is considered. Neglecting the scalar couplings $^1J_{CBr}$ and $^2J_{HBr}$ at zero order as well as those to the acidic ^{1}H, the spin system has an A$_2$X topology and the zero-field NMR spectrum is expected to contain a single resonance at a frequency of $1.5 \times\,^1J_{CH}$ [2].

The experimental line width of the zero-field NMR transitions were measured for 99% ^{13}CH$_2$BrCOOH dissolved to 8.0 mol.dm^{-3} in ^{13}CH$_3$COOH, see Figure 3. The acetic acid serves two purposes in this experiment: (i) to dissolve bromoacetic acid, which is a crystalline solid in pure form; (ii) as a reference peak in the zero-field NMR spectrum. Despite having a direct covalent bond to ^{13}C, and therefore a likely substantial J coupling, the bromine atom does not appear to significantly increase the zero-field line width. The peak at (231.30 ± 0.01) Hz ($^1J_{CH} \approx (154.113 \pm 0.007)$ Hz) has a width of 0.24 Hz, slightly broader than the 0.19 Hz width of the $^1J_{CH}$ peak for [2-^{13}C]-acetic acid. Assuming the same motional correlation time for each the

molecule, the difference of 0.05 Hz corresponds to an estimated bound $(^1J_{CBr})^2 T_2^{(S)} < 0.002$ s^{-1}, via Equation 4 with $S = 3/2$. This is in fair agreement with the value of around 0.001 s^{-1} calculated from parameters $^1J_{CBr} \sim 60$ Hz and $T_2^{(Br)} \sim 0.2\,\mu$s given in ref. [16].

4. Discussion and outlook

The above results show that for compounds containing rapidly-relaxing chlorine and bromine nuclei, SR2K is a negligible relaxation mechanism, conferring that the quadrupolar spin species in these molecules satisfy a weak coupling limit and a regime of rapid self decoupling where $J_{IS}^2 T_2^{(S)} \ll 1$ Hz. Both ultralow-field and zero-field NMR transitions involving ^{1}H and ^{13}C yielded highly resolved peak widths despite Cl/Br atoms in close proximity, including bromine directly bonded to ^{13}C. Since one-bond scalar couplings are much larger than those across multiple chemical bonds, the experimental result in Figure 3 may represent a worst case of SR2K between Br and ^{13}C at zero field.

The term "weak coupling" signifies that the effect of heteronuclear couplings on the spin system is well approximated by simple perturbation theory. The large disparity in relaxation rates (i.e. the real part of the
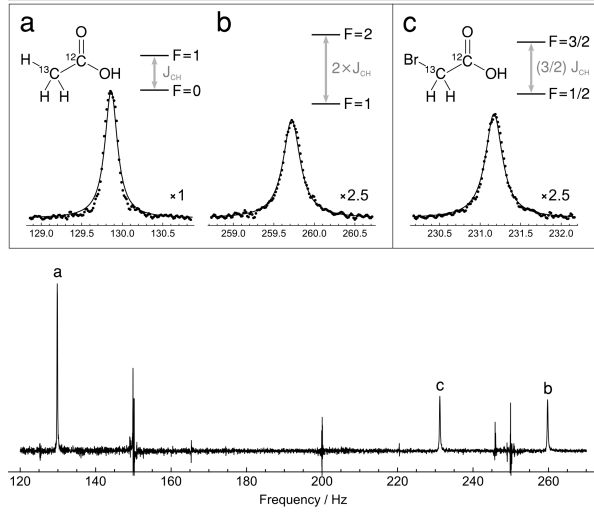
5

Figure 3: Zero-field NMR spectrum of [2-^{13}C]-bromoacetic acid dissolved in [2-^{13}C]-acetic acid (1:2 mole ratio). The horizontal axis gives the absolute signal frequency. Peak frequencies corresponding to multiples of ^{13}C-^{1}H scalar couplings are fitted as follows: (a) acetic acid $^1J_{CH}$ = 129.86(1) Hz; (b) acetic acid 2^1J_{CH} = 259.72(2) Hz; (c) bromoacetic acid $(3/2)^1J_{CH}$ = 231.30(1) Hz. These observable transitions occur between eigenstates of total angular momentum operator for the ^{1}H and ^{13}C nuclei, where the quantum number is denoted F and the selection rule is $|\Delta F| = 1$. Noise signals at multiples of 50 Hz are caused by the mains AC electricity supply to the instrument.

Liouvillian eigenvalues) between ^{1}H and Cl/Br is sufficient to meet the condition, even though the resonance frequencies (imaginary part of the Liouvillian eigenvalues) are small compared to heteronuclear scalar couplings [28]. This represents a situation of motion-induced spin decoupling that is independent of field strength. Therefore not all nuclei are strongly coupled at ultralow magnetic field, even at zero field.

Conversely, ^{1}H and ^{2}H may couple strongly to one another at low magnetic field due to similar relaxation rates of the nuclei, leading to resonance widths of several Hz at half maximum. Deuterium isotopic labeling of substrates is usually favored in high-field ^{1}H NMR to simplify spectral appearance and inhibit dipole-dipole relaxation. The present work shows that the presence of deuterium can broaden ^{1}H NMR transitions to a point that negates other advantages of the ultralow field regime for obtaining highly resolved NMR spectra. However, quadrupolar nuclei with relaxation rates that are comparable to those of ^{1}H or faster may be tolerated where J couplings are sufficiently small to fulfil the weak coupling condition, for example ^{14}N in [^{13}C]-acetonitrile (CH$_3$CN) [29, 30] or ^{2}H in ^{1}H$_2$O/^{2}H$_2$O mixtures [23].

In isotropic solution the relaxation rate of the quadrupole is given by

$$\frac{1}{T_2^{(S)}} = \frac{\pi^2 C_Q^2 (3 + \eta^2) \tau_c (2S + 3)}{10 S^2 (2S - 1)} \tag{5}$$

where $C_Q = e^2 Qq/h$ and η are the principal value and biaxiality of the nuclear quadrupole coupling tensor, respectively, and τ_c is the rotational correlation time of the molecule. In the expression for C_Q, Q is the electrical quadrupole moment of the nucleus, which is a fundamental property of each spin species. The other quantity, q, is the rotationally averaged gradient of electric field at the nucleus and depends on chemical bonding. Aside from geometric factors, the magnitude of J_{IS} is proportional to the magnitude of the nuclear magnetic dipole moments. As a result, nuclei with large quadrupole coupling constants ($^{35/37}$Cl, $^{79/81}$Br, ^{127}I) are most likely to give small values of the parameter $J_{IS}^2 T_2^{(S)}$, compared to nuclei with small quadrupole moments (^{2}H, ^{14}N, ^{17}O). This appears to be true for couplings to ^{1}H and ^{13}C over 1 or 2 chemical bonds. One exception is where the electric field gradient around the quadrupolar nucleus is totally symmetric under rotation, as in ^{14}NH$_4^+$ or $^{10/11}$BF$_4^-$. Equation 4 does not hold in these cases and the J_{IS} couplings should be spectroscopically resolved. Further studies of the crossover to strong coupling between spin-1/2 nuclei and quadrupolar nuclei near zero field ($J_{IS} \sim 1/T_2^S$), for instance where quadrupole coupling tensor is nearly spherically symmetric, should be greatly interesting in future work.

In summary, this work provides insight into the behavior of coupled heteronuclear spins at ultralow magnetic field, when one of the nuclear spin species has a nonzero quadrupole moment. On the one hand, spin couplings to quadrupolar nuclei may be embraced for they are a valuable source of information about molecular structure. On the other hand, it is also very important to know their impact upon (and possible detriment to) spectral resolution. The option to modify the spin topology by substituting ^{1}H nuclei with halogens (as demonstrated here for CH$_2$BrCOOH and CH$_3$COOH) without drastic increase in line width could enable new opportunities in many areas of NMR near zero field, including quantum information processing[31, 32] and a wider choice of substrates for hyperpolarization.

Appendix A. Perturbation solutions to the Liouville von Neumann equation

In the high-temperature low-ordering approximation the nuclear spin dynamics obeys the Liouville von-

Neumann master equation:

$$\mathrm{d}\sigma(t)/\mathrm{d}t \quad = \quad L[\sigma(t) - \sigma(\infty)], \qquad (A.1)$$

where $\sigma(t)$ is the nuclear spin density operator at time t and L is the Liouvillian superoperator. The Liouvillian comprises a coherent part, arising from the time-independent part of the spin Hamiltonian (H), plus a relaxation superoperator (Γ) arising from time-dependent interactions that are averaged under fast molecular motion:

$$L \quad = \quad -\mathrm{i}\hat{H} + \Gamma. \qquad (A.2)$$

Hat (^) denotes commutation superoperator. A stationary state of L, symbolized by the spin operator Q, is defined by the eigenvalue equation

$$LQ_j \quad = \quad -\lambda_j Q_j. \qquad (A.3)$$

By the definition $\mathrm{Tr}[Q_j^\dagger \rho(t)] = \mathrm{Tr}[Q_j^\dagger \rho(0)]\exp(-\lambda_j t)$, the real part of the eigenvalue $\mathrm{Re}[\lambda_j]$ corresponds to the relaxation rate of the spin order, while the imaginary counterpart $\mathrm{Im}[\lambda_j]$ gives the oscillation frequency.

For SR2K between I ($I = 1/2$) and S ($S > 1/2$) nuclei in the liquid state, Equation A.3 can be solved using perturbation theory provided that I-S coherences relax much faster than the magnitude of the I-S scalar coupling constant. Relaxation rates are calculated from a reference eigensystem (denoted by a superscript $^{(0)}$) where I-S scalar couplings are ignored and the relaxation is due to random reorientation of the S spin quadrupole tensor. Here the scalar coupling Hamiltonian is the perturbation term:

$$H_J = 2\pi J_{IS}\boldsymbol{I}\cdot\boldsymbol{S}, \qquad (A.4)$$

where J is the coupling constant in Hz. For a unique eigenvalue $\lambda_j^{(0)} = \mathrm{Tr}[Q_j^{(0)}\hat{H}Q_j^{(0)}]$ and eigenvector $Q_j^{(0)}$ the perturbed eigenvalue due to H_J is computed to second order as

$$\lambda_j \quad \approx \quad \lambda_j^{(0)} + \sum_{k\neq j}\lambda_k^{(0)}\left|\frac{\mathrm{Tr}[Q_k^{(0)}\hat{H}_J Q_j^{(0)}]}{\lambda_k^{(0)} - \lambda_j^{(0)}}\right|^2. \qquad (A.5)$$

The sum is taken over all other eigenoperators of the spin system. The real part of the correction term is positive, thus contributing to an increased relaxation rate. The imaginary part is known as the dynamic frequency shift, which is too small to be observed in the present experiments. The polarization of the I spin couples to bilinear spin operators of the same overall coherence order, leading to the rate expressions

$$\frac{1}{T_1^{(I)}} \quad = \quad \left[\left|\frac{\mathrm{Tr}[I_z^\dagger \hat{H}_J I_+ S_-]}{1/T_2^{(S)} + \mathrm{i}(\gamma_I - \gamma_S)B_z}\right|^2\right.$$

$$\left. + \left|\frac{\mathrm{Tr}[I_z^\dagger \hat{H}_J I_- S_+]}{1/T_2^{(S)} - \mathrm{i}(\gamma_I - \gamma_S)B_z}\right|^2\right]\frac{1}{T_2^{(S)}},$$

$$= \quad \frac{8\pi^2 J_{IS}^2}{3}\frac{S(S+1)T_2^{(S)}}{1 + (\gamma_I - \gamma_S)^2 B_z^2(T_2^{(S)})^2}, \qquad (A.6)$$

$$\frac{1}{T_2^{(I)}} \quad = \quad \left|\mathrm{Tr}[I_+^\dagger \hat{H}_J I_+ S_z]\right|^2 T_1^{(I)}$$

$$+ \left|\frac{\mathrm{Tr}[I_+^\dagger \hat{H}_J I_z S_+]}{1/T_2^{(S)} - \mathrm{i}(\gamma_I - \gamma_S)B_z}\right|^2\frac{1}{T_2^{(S)}},$$

$$= \quad \frac{4\pi^2 J_{IS}^2 S(S+1)}{3}T_1^{(I)} + \frac{1}{2T_1^{(I)}}. \qquad (A.7)$$

These correspond to Equations 1 and 2 in the main text. The assumption is that for $1/T^{(I)} \ll 1/T^{(S)}$, the coupled-spin order (e.g. $I_+ S_-$) relaxes at a rate $1/T^{(S)}$. Numerical modeling confirms that the two above equations accurately predict the result of full numerical propagation of the density operator, provided $1/|T^{(I)} - T^{(S)}| \gg 2\pi|J|$.

Also considered in this work is the NMR spectrum of a three-spin-species system IXS at zero field, where total angular momentum quantum numbers of each spin species are $I = X = 1/2$ and $S > 1/2$. An identical procedure to the above is followed to obtain the coherence decay rate due to SR2K. If $T_1^{(S)} \ll T_1^{(I/X)} \ll 2\pi|J_{IX}|$ then the zero-order eigensystem contains spin operators

$$Q_\pm \quad = \quad \frac{1}{2}\Big(I_+ X_- - I_- X_+ \pm (I_z - X_z)\Big) \qquad (A.8)$$

that oscillate at (eigen)frequencies of $\lambda_\pm/2\pi = \pm\mathrm{i}J_{IX}$ in Hz. These coherences are detectable with the magnetometer if the sensitive axis is parallel to z and $\gamma_I \neq \gamma_X$. Equation A.5 is used to obtain the second-order contribution to the eigenvalue via mixing of $Q_\pm$ with other zero-quantum spin operators $S_- I_+$, $S_+ I_-$, $S_- I_z X_+$, $S_+ I_- X_+$, $S_+ I_z X_-$ and $S_z I_+ X_-$, etc. The relaxation rate obtained is that given in Equation 4 of the main text:

$$\frac{1}{T^{(IX)}} \quad = \quad 2\pi^2(J_{IS}^2 + J_{XS}^2)S(S+1)T_2^{(S)}. \qquad (A.9)$$

Solutions to Equation A.1 can also be found by diagonalizing the matrix representation of L to obtain a set of orthonormal eigenoperators and corresponding eigenvalues. This procedure must be adopted where the perturbation approximation cannot be made.

Acknowledgment

References

[1] J. W. Blanchard and D. Budker, Zero- to Ultralow-Field NMR, *eMagRes*, (2016) 13951410.

[2] Butler, M., Ledbetter, M. P., Theis, T., Blanchard, J. W., Budker, D. and Pines, A., Multiplets at zero magnetic field: the geometry of zero-field NMR, *J. Chem. Phys.* 138 (2013), 184202-15.

[3] P. Volegov, M. Flynn, R. Kraus. P. Magnelind, A. Matlashov, P. Nath, T. Owens, H. Sandin, I. Savukov, L. Schultz, A. Urbaitis, V. Zotev and M. Espy, Magnetic resonance relaxometry at low and ultra low fields, *IFMBE Proc.* 28 (2010), 82-87.

[4] *Optical Magnetometry*, edited by D. Budker and D. F. Jackson Kimball (Cambridge University Press (2013), ISBN: 1107010357.

[5] A. H. Trabesinger, R. McDermott, S. Lee, M. Mück, J. Clarke and A. Pines, SQUID-detected liquid-state NMR in microtesla fields, *J. Phys. Chem. A* 108 (2004), 957-963.

[6] I. M. Savukov, M. V. Romalis, NMR detection with an atomic magnetometer, *Phys. Rev. Lett.* 94 (2005), 123001.

[7] M. C. D. Tayler, T. Theis, T. F. Sjolander, J. W. Blanchard, A. Kentner, S. Pustelny, A. Pines and D. Budker, Instrumentation for nuclear magnetic resonance in zero and ultralow magnetic field. *Rev. Sci. Instrum.* 88 (2017), 091101.

[8] R. V. Shchepin, L. Jaigirdar and E. Chekmenev, Spin-lattice relaxation of hyperpolarized metronidazole in signal amplification by reversible exchange in micro-tesla fields, *J. Phys. Chem. C* 122 (2018), 4984-4996.

[9] K. Buckenmaier, M. Rudolph, C. Back, T. Misztal, U. Bommerich, P. Fehling, D. Koelle, R. Kleiner, H. A. Mayer, K. Scheffler, J. Bernarding and M. Plaumann, SQUID-based detection of ultra-low-field multinuclear NMR of substances hyperpolarized using signal amplification by reversible exchange, *Sci. Rep.* 7 (2017), 13431.

[10] T. Theis, P. Ganssle, G. Kervern, S. Knappe, J. Kitching, M. P. Ledbetter, D. Budker and A. Pines, Parahydrogen-enhanced zero-field nuclear magnetic resonance, *Nat. Phys.* 7 (2011), 571-575.

[11] J. F. Colell, A. W. Logan, Z. Zhou, R. V. Shchepin, D. A. Barskiy, G. X. Ortiz Jr., Q. Wang, S. J. Malcolmson, E. Y. Chekmenev, W. S. Warren and T. Theis, Generalizing, extending and maximizing nitrogen-15 hyperpolarization induced by parahydrogen in reversible exchange, *J. Phys. Chem. C* 121 (2017), 6626-6634.

[12] A. Abragam, *The principles of nuclear magnetism*, Oxford, Clarendon Press, ISBN: 0198512368.

[13] D. A. Barskiy, R. V. Shchepin, C. P. N. Tanner, J. F. P. Colell, B. M. Goodson, T. Theis, W. S. Warren and E. Y. Chekmenev, The absence of quadrupolar nuclei facilitates efficient ^{13}C hyperpolarization via reversible exchange with parahydrogen, *ChemPhysChem* 18 (2017), 1493-1498,

[14] S. Hartwig, J. Voigt, H.-J. Scheer, H.-H. Albrecht, M. Burghoff and L. Trahms, Nuclear magnetic relaxation in water revisited, *J. Chem. Phys.* 135 (2011), 054201.

[15] V. Mlynárik, Measurement of spin coupling constants to quadrupolar nuclei via relaxation studies, *Progr. NMR Spectrosc.* 18 (1986), 277-305.

[16] S. Hayashi, K. Hayamizu and O. Yamamoto, Spin-spin coupling constants between carbon-13 and bromine and their correlations with the s character of the carbon hybridization, *J. Magn. Reson.* 37 (1980), 17-29.

[17] D. Kubica, A. Wodyński, A. Kraska-Dziadecka and A. Gryff-Keller, Scalar relaxation of the second kind. A potential source of information on the dynamics of molecular movements. 3. A ^{13}C nuclear spin relaxation study of CBrX$_3$ (X = Cl, CH$_3$, Br) molecules, *J. Phys. Chem. A* 118 (2014), 2995-3003.

[18] A. Briguet, J. C. Duplan and J. Delmau, Scalar relaxation of the second kind for ^{29}Si in SiCl$_4$ and SiHCl$_3$, *J. Magn. Reson.* 42 (1981), 141-146.

[19] J. Kowalewski, L. Mäler, *Nuclear spin relaxation in liquids, Second Edition*, CRC press (2017). ISBN: 9781351264587.

[20] I. M. Savukov, Spin Exchange Relaxation Free (SERF) Magnetometers. In: Grosz A., Haji-Sheikh M., Mukhopadhyay S. (eds) *Smart Sensors, Measurement and Instrumentation*, Springer book series, vol 19. (2016) 451-491.

[21] K. Omata, S. Aoyagi and K. Kabuto, Observing the enantiomeric ^{1}H chemical shift non-equivalence of several α-amino ester signals using tris[3-(trifluoromethylhydroxymethylene)-(+)-camphorato]-samarium(III): a chiral lanthanide shift reagent that causes minimal line broadening, *Tetrahedron: Asymm.* 15 (2004), 2351-2356.

[22] W. C. Lewis and B. E. Norcross, Average geminal and vicinal proton-deuterium coupling constants in variously deuterated ethanol, propanol-2 and toluene, *J. Org. Chem.* 30 (1965), 2866-2867.

[23] G. Bevilacqua, V. Biancalana, Y. Dancheva, A. Vigilante, A. Donate and C. Rossi, Simultaneous detection of H and D NMR signals in a micro-tesla field, *J. Chem. Phys. Lett.* 8 (2017), 6176-6179.

[24] M. Emondts, M. P. Ledbetter, S. Pustelny, T. Theis, B. Patton, J. W. Blanchard, M. C. Butler, D. Budker and A. Pines, Long-lived heteronuclear spin-singlet states in liquids at a zero magnetic field, *Phys. Rev. Lett.* 112 (2014), 077601.

[25] Ledbetter, M. P., Crawford, C. W., Pines, A., Wemmer, D. E., Knappe, S., Kitching, J. and Budker, D., Optical detection of NMR J-spectra at zero magnetic field, *J. Magn. Reson.* 199 (2009), 25-29.

[26] Blanchard, J. W., Ledbetter, M. P., Theis, T., Butler, M., Budker, D. and Pines, A., High-resolution zero-field NMR J-spectroscopy of aromatic compounds, *J. Am. Chem. Soc.* 135 (2013), 3607-3612.

[27] A. Wilzewski, S. Afach, J. W. Blanchard and D Budker, A method for measurement of spin-spin couplings with sub-mHz precision using zero- to ultralow-field nuclear magnetic resonance, *J. Magn. Reson.* 284 (2017), 66-72.

[28] S. Appelt, F. W. Häsing, U. Sieling, A. Gordji-Nejad, S. Glöggler and B. Blümich, Paths from weak to strong coupling in NMR, *Phys. Rev. A* 81 (2010), 023420.

[29] J. W. Blanchard, T. F. Sjolander, J. P. King, M. P. Ledbetter, E. H. Levine, V. S. Bajaj, D. Budker and A. Pines, Measurement of untruncated nuclear spin interactions via zero- to ultralow-field nuclear magnetic resonance, *Phys. Rev. B* 92 (2015), 220202(R).

[30] M. P. Ledbetter, T. Theis, J. W. Blanchard, H. Ring, P. Ganssle, S. Appelt, B. Blümich, A. Pines and D. Budker, Near-zero-field nuclear magnetic resonance, *Phys. Rev. Lett.* 107 (2011), 107601.

[31] M. Jiang, J. Bian, X. Liu, H. Wang, Y. Ji, B. Zhang, X. Peng and J. Du, Numerical optimal control of spin systems at zero magnetic field, *Phys. Rev. A* 97 (2018), 062118.

[32] M. Jiang, T. Wu, J. W. Blanchard, G. Feng, X. Peng and D. Budker, Experimental benchmarking of quantum control in zero-field nuclear magnetic resonance, *Science Adv.* 4 (2018), EEAR6327.